

# Optimising hybrid Fibre and nanocellulose reinforced engineered cementitious composites using Taguchi-TOPSIS analysis

H. Withana<sup>a</sup>, S. Rawat<sup>a,b</sup>, Y.X. Zhang<sup>a,c,\*</sup>

<sup>a</sup> School of Engineering, Design and Built Environment, Western Sydney University, NSW, 2751, Australia

<sup>b</sup> School of Civil and Environmental Engineering, University of Technology Sydney (UTS), Sydney, NSW, 2007, Australia

<sup>c</sup> School of Mechanical and Mechatronic Engineering, Faculty of Engineering and Information Technology, University of Technology Sydney, NSW, 2007, Australia

## ARTICLE INFO

### Keywords:

Engineered cementitious composites  
High volume fly ash  
Nanocellulose  
Optimization  
Taguchi method  
TOPSIS

## ABSTRACT

A structured approach to optimising the constituents of engineered cementitious composites (ECC) is crucial for reducing resource intensity and improving design efficiency. This study presents the design of a novel sustainable ECC that simultaneously achieves high strength and ductility, incorporating hybrid fibres, nanocellulose (NC), and high volumes of fly ash and silica fume. A novel approach utilising the hybrid application of Taguchi-Technique for Order of Preference by Similarity to Ideal Solution (TOPSIS) methods is adopted for the design, enabling systematic and precise adjustment of mix constituents and leading to optimized performance. The standard Taguchi orthogonal array, consisting of four factors, i.e. fly ash to silica fume ratio, water-to-binder ratio, fibre proportions, and nanocellulose dosage, was used to design the mix. The optimum combination of these constituents was determined to maximize five key response parameters: compressive strength, elastic modulus, flexural strength, tensile strength, and ultimate tensile strain. Results indicated that fly ash to silica fume ratio of 1:0.2, a water to binder ratio of 0.22, 1.5 % polyethylene +0.75 % steel fibre by volume, and 0.25 % NC by weight represent the optimal mix design. This mix achieved a compressive strength of 71 MPa, an elastic modulus of 30 GPa, a flexural strength of 17 MPa, an ultimate tensile strength of 4 MPa, and an ultimate tensile strain of 3 %. The optimal design was further validated by experimental results, which showed that the optimized mix outperformed all other mixes in all indices. This further demonstrates the effectiveness of the design method and the potential for successfully incorporating nanocellulose in ECC designs.

## 1. Introduction

Engineered cementitious composite (ECC) is a unique class of high-performance fibre reinforced cementitious composites that were developed to significantly improve strain hardening behaviour, addressing the issue of material brittleness. The development of ECC has undergone extensive research since its invention in the early 1990s [1]. It is well showcased that ECC can be tailored to meet specific functional requirements by carefully adjusting its constituents [2–5]. However, achieving an optimal balance between strength, ductility, and durability requires careful proportioning of multiple mix components, which becomes especially complex when targeting sustainability [6].

One of the major limitations of conventional ECC is its high cement content usage due to the absence of coarse aggregates. Although supplementary cementitious materials (SCMs) such as fly ash (FA) have been used to partially replace cement, use of high-volume fly ash

(HVFA) can lead to reduced early-age strength and compromised mechanical properties. Enhancing the sustainability of ECC without sacrificing strength or ductility remains a significant challenge.

Recent research has focused on introducing other kinds of SCMs such as silica fume (SF) and novel bio-based additives like nanocellulose (NC) to overcome the performance limitations of HVFA-based composites. Studies have shown that the high aspect ratio and specific surface area of NC promote strong bonding by increasing the availability of hydroxyl groups for hydrogen bonding with the cementitious matrix [7]. Furthermore, the hydrophilic and hygroscopic nature of NC facilitates internal curing, thereby enhancing the degree of hydration. These properties make NC promising for ECC containing high volumes of SCMs, where matrix refinement is critical [8]. In addition to matrix enhancement, NC also contributes to improving the fibre–matrix interactions. Combining macro steel fibres and micro polyethylene (PE) fibres offers a synergistic effect: steel fibres contribute to strength and

\* Corresponding author. School of Engineering, Design and Built Environment, Western Sydney University, NSW, 2751, Australia.

E-mail address: [Sarah.Zhang@uts.edu.au](mailto:Sarah.Zhang@uts.edu.au) (Y.X. Zhang).

<https://doi.org/10.1016/j.mtsust.2025.101224>

Received 22 July 2025; Received in revised form 30 August 2025; Accepted 20 September 2025

Available online 21 September 2025

2589-2347/© 2025 The Authors. Published by Elsevier Ltd. This is an open access article under the CC BY license (<http://creativecommons.org/licenses/by/4.0/>).

toughness, while PE fibres enhance ductility and crack control. The inclusion of NC adds a third, nano-scale level of reinforcement, modifying the interfacial properties and potentially further enhancing performance. Despite this, the combined use of macro (steel), micro (PE), and nano (NC) fibres in ECC is still in its infancy.

Nevertheless, designing such complex multi-fibre, multi-SCM composites using conventional trial-and-error approaches is highly inefficient due to the number of interacting variables. While numerous research has explored the individual effects of these factors, such as the effect of different fibre ratios of PE and steel [9], effect of fly ash to silica fume ratios [10], effect of varying NC dosages [8] and water to binder ratio [11], the combined effects of these factors have not been studied comprehensively. The challenge is further amplified when multiple performance metrics (e.g., compressive strength, tensile strength, tensile strain, modulus, and flexural strength) must be optimized simultaneously. A systematic and efficient approach is therefore essential to replace conventional and resource-intensive methods, and to improve the efficacy of ECC mix design.

To address these challenges, this study proposes the use of a multi-response optimization framework based on an integrated Taguchi–Technique for Order of Preference by Similarity to Ideal Solution (TOPSIS) method. The Taguchi method provides an efficient experimental design using orthogonal arrays, while TOPSIS facilitates the ranking of alternatives across multiple performance criteria. Despite its simplicity and robustness, this integrated approach has not yet been applied to the optimization of hybrid ECC incorporating nano (NC), micro (PE) and macro (steel) fibres. The process entails identifying the key factors that influence the ECC design, including the fly ash-silica fume ratio, PE-steel fibre ratio, NC dosage and water-binder ratio. Using the standard Taguchi orthogonal array ( $L_9$ ), these mix parameters are analysed for five response parameters, namely, compressive strength, ultimate tensile strength, ultimate tensile strain, elastic modulus, and flexural strength. Following this, the TOPSIS method, integrated with the Taguchi approach, is employed to determine the optimal mix for these five response parameters. The validity of the optimal mix is further confirmed through experimental results, highlighting the successful application of the Taguchi-TOPSIS method for designing NC-based hybrid ECCs. The method proposed is anticipated to assist future researchers in designing nano additive-based hybrid ECCs more effectively, enabling an advanced design process with enhanced efficacy, quality, and accuracy.

## 2. Materials and design methods

### 2.1. Selection of constituents and factors for the mix design

The key constituents used in this study are cement, sand, water, fly ash (FA), silica fume (SF), steel fibres, polyethylene (PE) fibres, and nanocellulose (NC). More than 50 % cement is replaced with fly ash to lower the carbon footprint. NC is employed to improve the denseness of the matrix, counteracting any potential reduction caused by the addition of HVFA, thereby improving the overall strength of the composite. Additionally, accompanying fly ash with silica fume has been reported in achieving a better balance between strength and strain [10,12]. Therefore, fly ash is combined with varying doses of silica fume to further optimize the mechanical performance. The hybrid application of low-modulus PE fibre and high-modulus steel fibre is employed to achieve an optimal balance between the strength and ultimate strain capacity of the ECC. Based on these mix constituents, four factors were determined namely fly ash: silica fume ratio, NC (wt.%), PE + steel fibre (vol%) and water-binder ratio, and are further outlined with their corresponding levels in Table 1.

#### 2.1.1. Fly ash-silica fume ratio (factor A)

In general, fly ash can delay the pre-mature fibre rupture and promote high ultimate strain capacity [3]. However, the elevated porosity

**Table 1**

Factors and corresponding levels.

Levels	Factors					
	A		B	C		D
	Fly ash	Silica fume	NC (wt. %)	PE (vol %)	Steel (vol %)	w/b ratio
1	1.2	0	0.20	1.25	1.00	0.26
2	1.1	0.1	0.15	1.50	0.75	0.30
3	1.0	0.2	0.25	1.75	0.50	0.22

and reduced matrix densification stemming from the spherical shape of fly ash particles can adversely affect the material's strength [3,13,14]. Therefore, fly ash is often accompanied with silica fume to achieve a better balance between strength and strain [10,12]. Silica fume as ultra-fine particles of silica, fills the voids between larger particles by making the interfacial zone denser [15]. However, it has been reported that beyond a certain point, adding excess silica fume only acts as a filler and may potentially hinder the properties [16]. Therefore, it is critical to optimize the ratio of fly ash to silica fume for achieving the desired balance between strength and strain. This ratio is considered a primary factor in the design and is tested at three levels: a high-volume fly ash mix (cement: fly ash = 1:1.2) with no silica fume, and two additional mixes where silica fume replaces 0.1 and 0.2 of the fly ash content.

#### 2.1.2. NC dosage (factor B)

The addition of NC in optimum quantities is critical, as too low quantities will be insufficient to bring the favourable properties, whereas too high quantities will cause agglomerations and can negatively affect the properties. Hence, determining the optimum concentration of NC that maximize the benefits of its use, especially when used with micro fibres, plays a significant role. Therefore, the NC percentage is selected as another key factor and evaluated at three levels: 0.15 %, 0.20 %, and 0.25 % by weight, based on findings from a previous study [17].

#### 2.1.3. PE-steel fibre ratio (factor C)

Fibres play a critical role in tailoring the design of ECC. High-modulus fibres, such as steel, contribute to high ultimate strength but lower strain capacity and smaller crack widths. In contrast, low-modulus fibres like PE increase strain capacity but result in lower ultimate strength and larger cracks [13]. Hence, hybridising ECC with low modulus fibre such as PE fibre and high modulus fibres such as steel fibres can simultaneously improve the ultimate strength, strain capacity and crack width properties [9]. Therefore, suitably balancing their quantities is vital to achieve the optimum strain hardening properties of the ECC. Thus, in this study, the PE-steel fibre combination is tested at three levels: 1.75 % PE + 0.5 % steel, 1.5 % PE + 0.75 % steel, and 1.25 % PE + 1 % steel, maintaining a constant total fibre volume of 2.25 %, as recommended in previous literature [9].

#### 2.1.4. Water-binder ratio (factor D)

Finally, maintaining the correct mix rheology and workability is essential to ensure proper fibre distribution and prevent fibre clustering. If the water to binder (w/b) ratio is too high, excess water remains unconsumed during hydration, creating microscopic pores that weaken the composite. Conversely, a low w/b ratio increases frictional bonding, which can hinder multiple cracking and strain-hardening behaviour [11]. Thus, it is important to maintain an optimal w/b ratio that supports both workability and the desired material properties. In this study, w/b ratio is also identified as a main factor and analysed at three different levels, ranging from 0.22 to 0.30, as detailed in Table 1.

### 2.2. Materials and properties

General purpose ordinary Portland cement conforming to AS-3972

[18], class F fly ash and high-grade silica fume are used as the binding material, while sand of mean grain size 225  $\mu\text{m}$  was used as fine aggregate. The sand/binder ratio was kept constant at 0.36 as recommended in Ref. [8]. The properties of PE and steel fibres are shown in Table 2. Cellulose Nanofibrils (CNF) from Cellulose Lab, Canada was used as the NC. It was received as a slurry in aqueous gel form with 3.0 % by weight. The material properties of the NC are shown in Table 3. Additionally, polycarboxylate-based high range water reducer (HRWR) Rheobuild 10000N7 was used, and its dosage were varied to attain sufficient workability for uniform fibre dispersion.

### 2.3. Optimal mix design

The optimal mix design is determined using the four factors, fly ash/silica fume ratio, NC dosage, PE-steel fibre ratio, and water-binder (w/b) ratio, each of which have three levels as shown in Table 1. A simple logic when laying out a study of this nature would be to establish all possible combinations of factors along with appropriate ranges (levels) of each of the factors. However, the total number of combinations would be excessively large; for example, investigating four factors at three levels each as adopted in this study would require 81 ( $3^4$ ) trials. Therefore, a standard  $L_9$  Taguchi orthogonal array (OA) is used to efficiently reduce the number of trials to nine as shown in Table 4. Here A, B, C and D represents the four selected factors: fly ash/silica fume ratio, NC dosage (wt %), PE and steel fibre content, and the w/b ratio, as described in Section 2.1. Compressive, tensile, and flexural properties are investigated for each mix and five response parameters viz, compressive strength, ultimate tensile strength, ultimate tensile strain, elastic modulus and flexural strength were obtained. Thereafter, TOPSIS method integrated with the Taguchi method is used to analyse the optimal mix design that maximises these five parameters. The procedures of design of experiments are summarised in Fig. 1.

### 2.4. Specimen casting and testing

The specimens were casted by following the mixing and curing procedures adopted in a previous study [8]. A series of uniaxial compressive, elastic modulus, uniaxial tensile and four-point bending tests were carried out on the nine mixes. The compression and Young's modulus tests were conducted using an Instron universal testing machine with a 1000 kN capacity, following the Australian Standard AS 1012 [19]. Compressive tests were conducted on 50 mm cubes at a loading rate of 20 MPa/min, while 100 mm diameter  $\times$  200 mm height cylinders were used to perform Young's modulus test. Dog-bone specimens with a cross-sectional area of 30 mm  $\times$  13 mm in the reduced section and a gauge length of 80 mm were used for the uniaxial tension test, and the tests were carried under displacement control at a loading rate of 0.01 mm/min. Four-point bending tests were conducted out on 350 mm  $\times$  50 mm  $\times$  50 mm prisms under displacement control at a loading rate of 0.01 mm/min [5].

## 3. Results and discussions

### 3.1. Experimental observations

The average values of the five response parameters obtained from the experimental results of the nine trials are presented in Table 5. Fig. 2 further displays the average values of the response parameters at different factor levels. However, it should be noted that these

**Table 2**  
Properties of micro fibres.

Fibre type	Diameter ( $\mu\text{m}$ )	Length (mm)	Young's Modulus (GPa)	Tensile Strength (MPa)	Density ( $\text{g}/\text{cm}^3$ )	Aspect Ratio	Shape
PE	24	12	116	3000	0.97	500	Straight
Steel	200 $\pm$ 3	13 $\pm$ 1	200	2500	7.8	80	Straight

**Table 3**

Dimensions and mechanical properties of the NC.

Type of NC	CNF-Slurry-SMC (Unmodified)
<b>Morphology</b>	Aqueous gel slurry-1-3 % solids in water
<b>Fibre Diameter</b>	30–80 nm
<b>Fibre Length</b>	Up to several hundred microns
<b>Fibre Density</b>	1.0 $\text{g}/\text{cm}^3$
<b>Surface group</b>	Hydroxyl hydrophilic

**Table 4**

Mix proportions as per Taguchi orthogonal  $L_9$  array.

Group	Mix No.	A (cement: Fly ash: silica fume)	B (NC wt.%)	C (Fibre vol%)		D (w/b ratio)
				PE (vol %)	Steel (vol%)	
A1B1C1D1	M1	1: 1.2: 0	0.20	1.25	1.00	0.26
A1B2C2D2	M2	1: 1.2: 0	0.15	1.50	0.75	0.30
A1B3C3D3	M3	1: 1.2: 0	0.25	1.75	0.50	0.22
A2B1C2D3	M4	1: 1.1: 0.1	0.20	1.50	0.75	0.22
A2B2C3D1	M5	1: 1.1: 0.1	0.15	1.75	0.50	0.26
A2B3C1D2	M6	1: 1.1: 0.1	0.25	1.25	1.00	0.30
A3B1C3D2	M7	1: 1.0: 0.2	0.20	1.75	0.50	0.30
A3B2C1D3	M8	1: 1.0: 0.2	0.15	1.25	1.00	0.22
A3B3C2D1	M9	1: 1.0: 0.2	0.25	1.50	0.75	0.26

observations reflect only the primary effects of each individual factor and the general trends of their influence, rather than the interaction effects between factors. A detailed discussion of the behaviour of each factor and the trends observed is provided in the following section.

#### 3.1.1. Fly ash/silica fume ratio

As observed in Fig. 2, reducing fly ash content and increasing silica fume content improved compressive strength, tensile strength, elastic modulus, and flexural strength while decreasing the ultimate tensile strain. This trend can be attributed to the increase and reduction in matrix densification arising from the ultra-fine silica fume particles and the spherical fly ash particles respectively, as observed in other studies [3,20]. Due to the large particle size, fly ash increases porosity of the composite and decreases the matrix/interface bond and matrix toughness [3]. On the other hand, the ultra-fine particles of silica fume fill the voids and densify the interfacial zone increasing composite strength [20]. Thus, high fly ash and low silica fume content result in weaker fibre/matrix bonds and lower strength, while lower fly ash and higher silica fume content increase matrix density and strength.

However, the weaker fibre-matrix interfacial bond resulting from higher fly ash content appears to enhance strain capacity. The low matrix toughness aids strain hardening in ECC by satisfying the energy criterion [3]. If the interfacial bond between fibre and matrix is too strong, the fibres can rupture prematurely. Due to the spherical shaped particles in fly ash, it acts like a smooth filler and reduces the chemical bond between the fibre and matrix, minimising the pre-mature fibre rupture [3]. Therefore, increased fly ash content favours strain hardening, resulting in higher strain capacities.

#### 3.1.2. Nanocellulose dosage

When the nanocellulose (NC) dosage was increased from 0.15 % to 2.5 %, the compressive strength, tensile strength, elastic modulus, and flexural strength reached an optimum value at 0.20 % NC. The

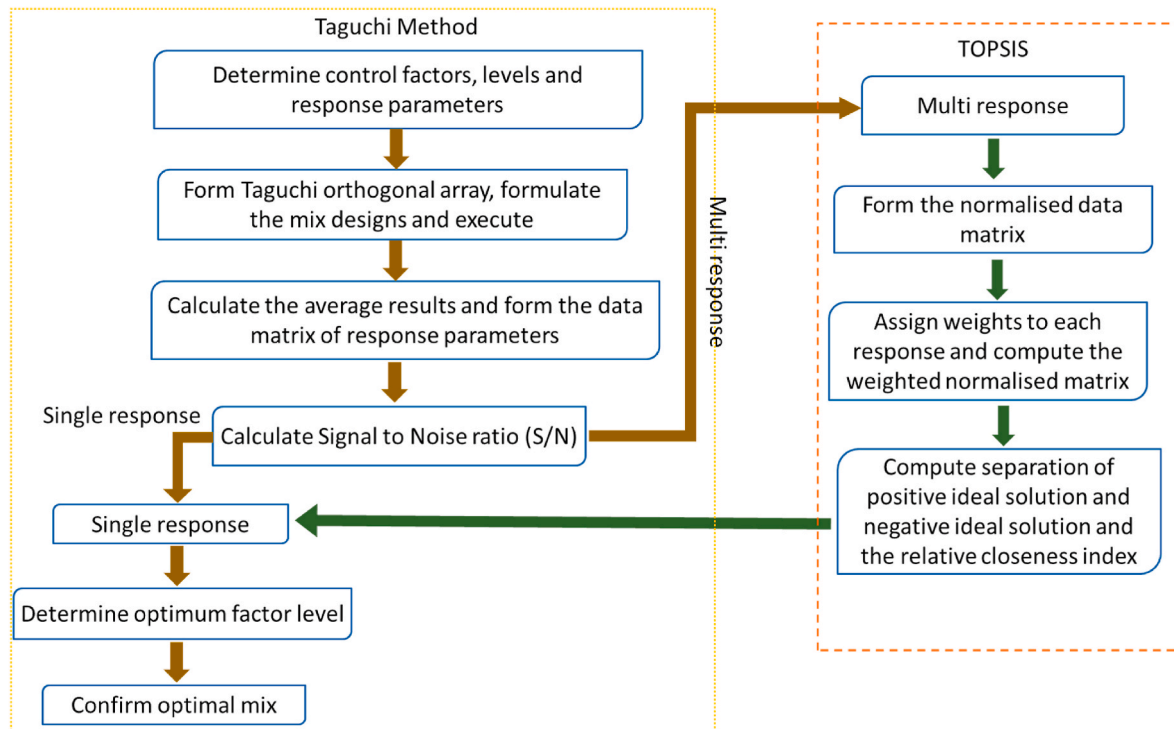


Fig. 1. Flowchart outlining the systematic approach for the hybrid TOPSIS Taguchi method.

Table 5

Average value of the responses of the L<sub>9</sub> OA mixes.

Mix No	Compressive Strength (MPa)	Elastic Modulus (GPa)	Flexural Strength (MPa)	Tensile Strength (MPa)	Ultimate Tensile Strain (%)
M1	62.52	25.42	14.43	3.67	2.40
M2	47.38	22.88	11.87	3.60	3.55
M3	61.16	28.26	13.76	4.80	2.67
M4	69.71	31.16	17.61	5.04	1.25
M5	57.38	23.64	14.47	4.67	2.70
M6	52.63	22.75	14.78	3.63	3.70
M7	56.94	27.61	15.88	3.87	2.13
M8	68.06	26.40	15.23	3.45	2.45
M9	71.48	30.12	16.42	3.70	2.80

enhancement in strength when NC% increased from 0.15 % to 0.20 % could be attributed to the strong bonding resulting from NC, whilst the reduction in strength at 0.25 % of NC could be attributed to fibre agglomeration arising from difficulty of dispersion. However, a negative correlation was observed between strength and strain since matrix densification could potentially limit strain capacity and favour strength. The reduced porosity in the mixes with NC relative to the reference mix may have led to the enhanced degree of hydration resulting from the internal curing effect of NC. Moreover, the high aspect ratio and the high specific surface area of NC might also have promoted the strong bonding by availing more hydroxyl groups to hydrogen bond with the cementitious matrix as observed in previous studies [7]. Though these factors improve strength, they may adversely affect strain properties.

### 3.1.3. PE/steel fibre ratio

All the measured response parameters-compressive strength, tensile strength, elastic modulus and flexural strength, reached an optimum at 1.5 % PE and 0.75 % steel fibre ratio. An increase in these properties as the PE content increased to 1.5 % and a decline with any further addition of PE was also reported in other studies [5,9], which could be attributed to the difficulty in fibre dispersion. Furthermore, the observed increase in strength with an increase in steel fibre content from 0.5 % to

0.75 % has also been confirmed by other studies [9,21], and is likely due to the high modulus of steel. Ultimate tensile strain continued to increase as the PE content increased from 1.25 % to 1.75 %, which can be attributed to the fibre bridging of PE fibres as confirmed by other studies [5,9]. In contrast, increase in steel fibre volume showed a negative effect on ultimate tensile strain. Similar behaviour was observed in other studies [5] while some reported that there was no clear relationship between tensile strain capacity and volume fractions of steel fibres [9]. Thus, it can be concluded that the low modulus of PE contributes to enhancement in strain while the high modulus steel fibres contribute to improving strength. However, there is a maximum volume fraction of fibres in total beyond which no improvement in tensile hardening occurs, likely due to poor dispersion of fibres caused by their excessive amount [9].

### 3.1.4. Water-binder ratio

Increasing the water-binder (w/b) ratio from 0.22 to 0.30 led to reduced compressive strength, tensile strength, elastic modulus, and flexural strength. A negative effect on the above properties of higher w/b ratio was also reported in other studies [5,22], which was attributed to the more porous and weaker bonding strength of the steel fibre/matrix stemming from the increased w/b ratio. On the contrary, a negative correlation was observed between ultimate tensile strain and the w/b ratio, which can be explained by the weaker fibre/matrix bonding favouring the strain [11].

## 3.2. Analysis of results

Although the main effects of each of the factors were identified from the nine experimental trials, it is important to note that the Taguchi method represents only a subset of a full factorial design. Consequently, the optimal condition may not necessarily be among these nine trials. Therefore, the best combination of factor-levels that gives the optimum condition is estimated. This is done by converting the five multiple response problem into a single response problem by integrating Taguchi method with TOPSIS method as outlined below.



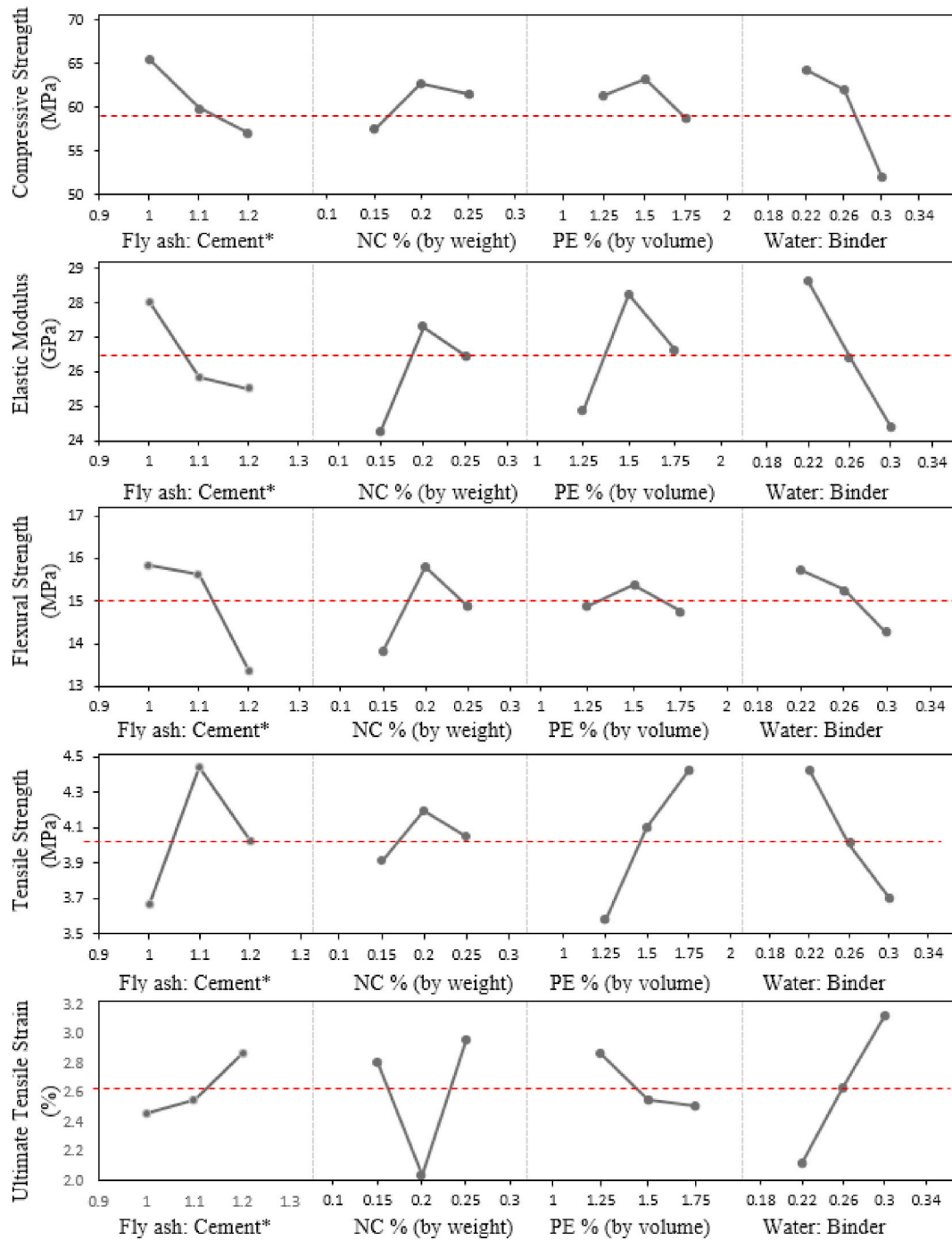


Fig. 2. Mean response of the main effect of different factors at three levels.

\*Fly ash: silica fume ratios of 1:0.2, 1.1:0.1, and 1.2:0 are represented by fly ash: cement ratios of 1, 1.1, and 1.2, respectively.

### 3.2.1. Signal-to-noise (S/N) analysis

First, the average values of the five response parameters from the nine trials (given in Table 5) are transformed into S/N ratios using Equation (1).

$$S/N \text{ ratio} = -10 \log_{10}(MSD), \quad (1)$$

where MSD represent the mean square deviation for “the higher the better” quality characteristic and can be calculated using Equation (2).

$$MSD = \sum_{i=1}^n \frac{1}{y_i^2}, \quad (2)$$

where  $n$  is the number of trials and  $y_i$  is the response characteristic of the  $i^{th}$  experiment in the OA. S/N ratios are essentially a scale transformation of raw data for easier manipulation. When an experiment includes multiple trials, converting the raw results to S/N ratios simplify the analysis. This approach helps determine the relative significance of the factors by evaluating the minimum variance considering the average value and the standard deviation of the test results simultaneously [5,23,24].

### 3.2.2. Normalisation

Next, each column of S/N is normalized using Equation (3) [25]. The normalized data matrix, ranging from 0 to 1 was obtained using the

benefit criteria of Linear max-min normalisation measurements and is presented in Table 6. This step is necessary to convert all the measurements of the five response parameters into a non-dimensional form and to eliminate distortion caused by different measurement scales.

The element  $r_{ij}$  of the normalized matrix is given by,

$$r_{ij} = \frac{x_{ij} - x_{j,\min}}{x_{j,\max} - x_{j,\min}}, i = 1, \dots, n; j = 1, \dots, m, \quad (3)$$

where  $r_{ij}$  is the element  $(i, j)$  of the normalized matrix  $x_{j,\max} = \max\{x_j\}$ ,  $x_{j,\min} = \min\{x_j\}$ ,  $n$  is the number of trials,  $m$  is the number of response parameters and  $x_{ij}$  is the S/N ratio of the response parameter  $j$  in the  $i$ th trial.

### 3.2.3. Weighted normalized decision matrix

The third step is to calculate the weighted normalized ratings of the normalized data matrix to ensure that each parameter (measurement) is represented proportionately. This was done by assigning equal weights to all the response parameters, using Equation (4).

The element  $w_{ij}$  of the weighted normalized matrix is given by

$$w_{ij} = \frac{1}{m} r_{ij}, \quad (4)$$

where  $m$  is the number of response parameters.

### 3.2.4. Determination of the ideal solution

The separation from the positive ideal solution (PIS) and negative ideal solution (NIS) is a critical step in the TOPSIS method where PIS represents the best possible value, while NIS represents the worst possible value for each response parameter from the nine trials. To estimate this, the distance of each result from the PIS and NIS is calculated using Equations (5) and (6) respectively [23]. These values are then used to determine the relative closeness or the ranking score using Equation (7). A higher value indicates that the alternative is closer to the PIS and farther from NIS making it more desirable. This process ensures that the chosen result is not only close to the ideal but also far from the worst-case scenario and helps in making balanced decisions. Thus, the selected result is robust and desirable across all response variables [23, 26, 27].

The distance from the positive ideal solution of the  $i$ th trial  $S_i^+$  is given by,

$$S_i^+ = \sqrt{\sum_{j=1}^m (w_{ij} - w_j^*)^2}, \quad (5)$$

where  $w_j^* = \max\{w_j\}$ .

The distance from the negative ideal solution of the  $i$ th trial  $S_i^-$  is given by,

$$S_i^- = \sqrt{\sum_{j=1}^m (w_{ij} - w_j')^2}, \quad (6)$$

where  $w_j' = \min\{w_j\}$ .

The ranking score  $C_i$  of the  $i$ th trial is given by,

$$C_i = \frac{S_i^-}{S_i^- + S_i^+} \quad (7)$$

The ranking score,  $C_i$ , calculated as per Equation (7) and its respective rank is presented in Table 7.

### 3.2.5. Determining the optimum mix

Finally, the optimal mix is calculated via the Taguchi method using the  $9 \times 1$  matrix obtained through TOPSIS. Although, it can be observed that trial 9, corresponding to A3B3C2D1, ranks highest in the analysis, it cannot be conclusively identified as the optimal mix because only a single value of each response parameter has been considered in this calculation. To accurately determine the optimal mix, it is necessary to analyse the mean effect of each factor on the response parameters. This involves calculating the mean responses of each factor at every level, obtained by averaging the results of all trials corresponding to the level being analysed. The average values for each factor level are presented in Table 8. From these averages, the level that gives the highest average for each factor is identified. As can be seen from Table 8, the optimum combination was found to be A3B3C3D3. The main effect of the factors on overall responses, based on the ranking score is further depicted in Fig. 3.

It can be observed that the lowest w/b ratio and highest fly ash to silica fume ratio contributed to the optimum performance, aligning with the behaviour observed when these factors were considered individually, as discussed in Section 3.1. However, the fibre content that optimises performance differs when the effects of the factors are considered in combination. The optimal proportion after combining all the response parameters into a single index appears to be 1.75 vol% PE + 0.5 vol% steel + 0.25 wt% NC, whereas the optimal values when considered individually were 1.5 vol% PE + 0.75 vol% steel + 0.2 wt% NC. It is possible that lowering the steel quantity may facilitate better PE and NC dispersion, and the fibre/matrix interaction is likely affected by the presence of other fibres. Nevertheless, the interaction between the micro fibres and nano fibres was not investigated in this study and future research is necessary to provide a more definitive explanation. It can further be deduced that the presence of NC affects the behaviour of micro fibres, and vice versa. Therefore, the combined effect should be considered when designing ECCs with multiple fibre types, particularly, micro, and nano fibres, as demonstrated in the present study.

### 3.2.6. Predicting the optimum responses

The trial mix corresponding to this optimal combination (A3B3C3D3) was not included in the experimentation program designed by Taguchi OA ( $L_9$ ). Therefore, optimal responses are calculated numerically by applying the balanced feature of the OA [5]. The Taguchi approach uses Equation (8) [28] to calculate the optimum responses and Equation (9) [28] to estimate the expected performances with a confidence interval.

The optimum value ( $Y_{opt}$ ) is calculated using,

**Table 6**

Normalized data matrix of the five response parameters.

Mix No	Compressive Strength (MPa)	Elastic Modulus (GPa)	Flexural Strength (MPa)	Tensile Strength (MPa)	Ultimate Tensile Strain (%)
M1	0.67	0.16	0.50	0.35	0.60
M2	0.00	0.11	0.00	0.02	0.96
M3	0.62	0.87	0.37	0.69	0.70
M4	0.94	1.00	1.00	1.00	0.00
M5	0.47	0.80	0.50	0.12	0.71
M6	0.26	0.13	0.56	0.00	1.00
M7	0.45	0.30	0.74	0.62	0.49
M8	0.88	0.00	0.63	0.47	0.62
M9	1.00	0.18	0.82	0.89	0.74

**Table 7**

Ranking scores and the rank of the mixes.

Mix No.	Ranking score	Rank
M1	0.462	7
M2	0.333	9
M3	0.636	3
M4	0.663	2
M5	0.516	6
M6	0.427	8
M7	0.517	4
M8	0.516	5
M9	0.665	1

**Table 8**

Average ranking scores of each factor at each level.

Factor		1	2	3
Fly ash/silica fume	A	0.476969	0.53518	<b>0.566065</b>
NC (wt %)	B	0.547321	0.454934	<b>0.575959</b>
PE-Steel (vol %)	C	0.468276	0.553855	<b>0.556082</b>
w/b	D	0.547692	0.425755	<b>0.604767</b>

$$Y_{opt} = \bar{T} + \sum_{i=1}^k (\bar{y}_i - \bar{T}), \quad (8)$$

where  $\bar{T} = \sum_{i=1}^n y_i / n$ , and  $n$  is the number of trials,  $k$  is the number of factors and  $\bar{y}_i$  is the factor average at  $i$ th factor level, which was obtained by adding the results of all trials at the level considered.

The confidence interval (C.I) is calculated using,

$$C.I = \bar{T} \pm \sqrt{\frac{F_{\alpha}(f_1, f_2) \times V_e}{n_e}}, \quad (9)$$

where  $F_{\alpha}(f_1, f_2)$  is the variance ratio for DOF at the level of significance  $\alpha$ , for a confidence level of  $(1 - \alpha)$ ,  $f_1 = \text{DOF of mean} = 1$ ,  $f_2 =$ , DOF of error term  $V_e =$  variance of error term,  $n_e =$  Number of equivalent replications. The optimal settings of performance parameters and the estimated values at a 95 % confidence interval are presented in Table 9. These predicted results were validated by performing a confirmation experiment.

### 3.3. Confirmation experiment

After the optimum condition was determined and expected performance (predicted value) was estimated, a confirmation experiment was performed to verify the projections. This step is necessary to validate the assumptions used in the analysis. The average values of five responses parameters obtained from the confirmation trials are given in Table 10. Additionally, the tensile stress-strain behaviour of the three most consistent results out of the six specimens tested during the confirmation experiments are depicted in Fig. 4.

The confirmation trial test results (Table 10) of all response parameters fell within respective 95 % confidence interval (Table 9) demonstrating the accuracy and reliability of the model. The compressive strength  $70.47 \pm 2.2$  MPa, achieved in the confirmation trial, is in close agreement with the predicted value of 71.00 MPa and falls within the confidence interval of 61.89–80.10 MPa. Similarly, the elastic modulus observed at  $29.40 \pm 3.1$  GPa closely aligns with the predicted value of 30.20 GPa, falling well within its interval of 24.83–35.56 GPa. The tensile strength, recorded as  $4.18 \pm 0.5$  MPa, also lies well within the predicted range of 3.51–4.52 MPa while the ultimate tensile strain of  $2.73 \pm 0.3$  %, aligns well with the predicted value of 3.06 % and falls within the interval of 2.55–3.56 %. The flexural strength from

confirmation trial was  $16.8 \pm 1.8$  MPa, slightly lower than the predicted optimum value of 17.47 MPa. However, with a confidence interval of 16.28–18.67 MPa, the experimental result remains within the expected range. This suggests that the minor deviation is within acceptable experimental variability, potentially influenced by the inconsistency in the fibre distribution or specimen casting. Consequently, it can be deduced that the mix comprising of 1:0.2 fly ash to silica fume ratio, 0.22 of water binder ratio, 1.75 % PE + 0.5 % steel fibre by volume and 0.25 % NC by weight is the optimum combination. This combination effectively achieves the benefits of using both nano (NC) and micro (PE-

**Table 9**

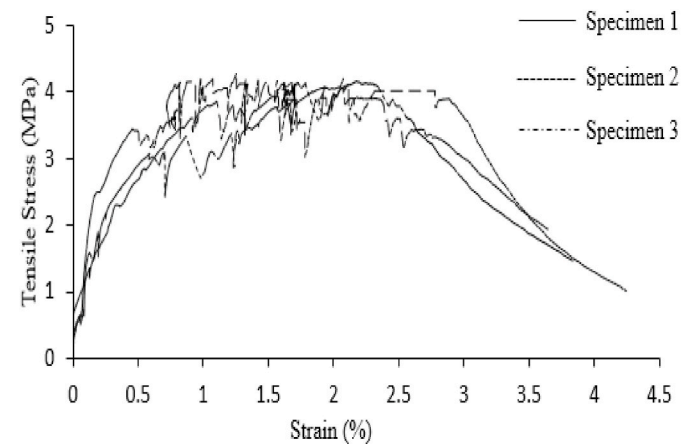
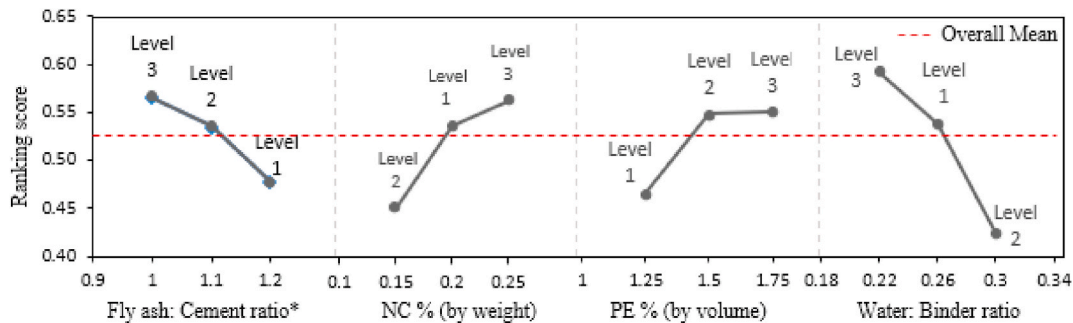
Optimal setting of the performance attributes.

Parameter	Predicted optimum value	95 % confidence interval
Compressive Strength (MPa)	71.00	[80.10-61.89]
Elastic Modulus (GPa)	30.20	[35.56-24.83]
Flexural Strength (MPa)	17.47	[18.67-16.28]
Tensile Strength (MPa)	4.01	[4.52-3.51]
Ultimate Tensile Strain (%)	3.06	[3.56-2.55]

**Table 10**

Response parameters corresponding to confirmation trail.

Parameter	Average response
Compressive Strength (MPa)	$70.47 \pm 2.2$
Elastic Modulus (GPa)	$29.40 \pm 3.1$
Flexural Strength (MPa)	$16.8 \pm 1.8$
Tensile Strength (MPa)	$4.18 \pm 0.5$
Ultimate Tensile Strain (%)	$2.73 \pm 0.3$

**Fig. 4.** Tensile Stress strain behaviour of the confirmation experiments.**Fig. 3.** Main effect of the factors on overall responses.

\*Fly ash: silica fume ratios of 1:0.2, 1.1:0.1, and 1.2:0 are represented by fly ash: cement ratios of 1, 1.1, and 1.2, respectively.

steel) fibres, along with a high volume of supplementary cementitious materials.

#### 4. Conclusions

This study utilizes integrated Taguchi-TOPSIS method to develop a novel nanocellulose reinforced hybrid ECC. The ECC was designed by hybridizing micro (polyethylene-steel) and nano (NC) scale fibres to achieve high strength and ductility simultaneously. Additionally, fly ash and silica fume were utilized as supplementary cementitious materials to reduce cement usage and enhance sustainability. The optimum factor-level combination that simultaneously maximises the multiple parameters, viz, compressive strength, Young's modulus, flexural strength, tensile strength, and tensile strain, was determined by employing a multi-attribute decision making method, TOPSIS, integrated with Taguchi analysis. The contribution of this study lies in its novel integration of methodical optimization techniques and sustainable materials, offering a significant advancement in the field of high-performance, sustainable construction materials.

The following key conclusions were drawn from the study.

- As the fly ash content decreased and the silica fume content increased from 1.2:0 to 1.0:0.2, compressive strength, tensile strength, elastic modulus, and flexural strength improved. However, a decrease in these properties was observed when the w/b ratio increased from 0.22 to 0.30.
- Thresholds for PE, steel, and NC were identified at 1.5 vol%, 0.75 vol %, and 0.2 wt%, respectively, beyond which strength parameters and elastic modulus began to decline. In contrast, a negative correlation was observed between ultimate tensile strain and strength or elastic modulus.
- ECC with fly ash to silica fume ratio of 1:0.2 and water binder ratio of 0.22 when combined with 1.5 % PE and 0.75 % steel fibre by volume and 0.25 % NC by weight was found to be the optimum combination. This optimum mix achieved compressive strength of 71 MPa, Young's modulus of 30 GPa, flexural strength of 17 MPa, ultimate tensile strength of 4 MPa, and an ultimate tensile strain capacity of approximately 3 %.
- The confirmation trial demonstrated that all measured response parameters fell within their respective 95 % confidence intervals, thereby validating the accuracy and reliability of the optimization framework.

It is expected that the approach presented in this study will benefit future researchers in designing specific purpose ECCs more effectively, supplementing traditional, resource-intensive methods. Nevertheless, the interaction between each of the factors was not investigated in this study, which can be a focus for future research.

#### CRedit authorship contribution statement

**H. Withana:** Writing – review & editing, Visualization, Methodology, Investigation, Formal analysis, Data curation, Conceptualization. **S. Rawat:** Writing – review & editing, Supervision, Methodology, Conceptualization. **Y.X. Zhang:** Writing – review & editing, Supervision, Resources, Project administration, Methodology, Conceptualization.

#### Declaration of competing interest

The authors declare that they have no known competing financial interests or personal relationships that could have appeared to influence

the work reported in this paper.

#### Data availability

Data will be made available on request.

#### References

- [1] V.C. Li, On engineered cementitious composites (ECC) a review of the material and its applications, *J. Adv. Concr. Technol.* 1 (3) (2003) 215–230.
- [2] S. Wang, V. Li, Materials design of lightweight PVA-ECC. *Proceedings of HPFRCC*, 2003, pp. 379–390.
- [3] S. Wang, V.C. Li, Engineered cementitious composites with high-volume fly ash, *ACI Mater. J.* 104 (3) (2007) 233.
- [4] C. Lee, et al., Compressive performance of ECC-concrete encased high strength steel composite columns, *Eng. Struct.* 213 (2020) 110567.
- [5] S. Rawat, Y. Zhang, C. Lee, Multi-response optimization of hybrid fibre engineered cementitious composite using Grey-Taguchi method and utility concept, *Constr. Build. Mater.* 319 (2022) 126040.
- [6] V.C. Li, E.-H. Yang, Self healing in concrete materials, in: *Self Healing Materials*, Springer, 2007, pp. 161–193.
- [7] H. Withana, S. Rawat, Y. Zhang, Effect of nanocellulose on mechanical properties of cementitious Composites—A review, *Advanced Nanocomposites* 1 (1) (2024) 201–216.
- [8] H. Withana, et al., Engineered cementitious composite with nanocellulose and high-volume fly ash, *Constr. Build. Mater.* 451 (2024) 138849.
- [9] S. Ahmed, M. Maalej, Tensile strain hardening behaviour of hybrid steel-polyethylene fibre reinforced cementitious composites, *Constr. Build. Mater.* 23 (1) (2009) 96–106.
- [10] S. Zhu, Y. Zhang, C. Lee, Polyethylene-steel fibre engineered cementitious composites for bridge link slab application, *Structures* 32 (2021) 1763–1776.
- [11] Y. Yang, et al., Effects of water/binder ratio on the properties of engineered cementitious composites, *J. Wuhan Univ. Technol.-Materials Sci. Ed.* 25 (2) (2010) 298–302.
- [12] S. Zhu, Y. Zhang, C. Lee, Polyethylene-steel fibre engineered cementitious composites for bridge link slab application, *Structures* (2021).
- [13] S.F.U. Ahmed, M. Maalej, P. Paramasivam, Flexural responses of hybrid steel-polyethylene fibre reinforced cement composites containing high volume fly ash, *Constr. Build. Mater.* 21 (5) (2007) 1088–1097.
- [14] M. Şahmaran, V.C. Li, Durability properties of micro-cracked ECC containing high volumes fly ash, *Cement Concr. Res.* 39 (11) (2009) 1033–1043.
- [15] G. Long, X. Wang, Y. Xie, Very-high-performance concrete with ultrafine powders, *Cement Concr. Res.* 32 (4) (2002) 601–605.
- [16] S. Bhanja, B. Sengupta, Influence of silica fume on the tensile strength of concrete, *Cement Concr. Res.* 35 (4) (2005) 743–747.
- [17] H. Withana, Y.X. Zhang, Behavior of hybrid engineered cementitious composites containing nanocellulose, in: *Nanotechnology in Construction for Circular Economy*, Proceedings of NICOM7, 31 October-02 November, 2022, Melbourne, Australia, 2023, pp. 37–41.
- [18] S. Australia, As 3972 General Purpose and Blended Cements, Standards Australia, Sydney, Australia, 2010.
- [19] S. Australia, Methods of Testing Concrete, 2014, pp. 1012–1014. Sydney, SA.
- [20] M. Nili, V. Afroughsabet, The long-term compressive strength and durability properties of silica fume fiber-reinforced concrete, *Mater. Sci. Eng., A* 531 (2012) 107–111.
- [21] M. Khan, Y. Zhang, C. Lee, Mechanical properties of high-strength steel-polyvinyl alcohol hybrid fibre engineered cementitious composites, *Journal of Structural Integrity and Maintenance* 6 (1) (2021) 47–57.
- [22] Y. Wang, et al., Effect of polyethylene fiber content on physical and mechanical properties of engineered cementitious composites, *Constr. Build. Mater.* 251 (2020) 118917.
- [23] B. Şimşek, Y.T. İç, E.H. Şimşek, A TOPSIS-based Taguchi optimization to determine optimal mixture proportions of the high strength self-compacting concrete, *Chemometr. Intell. Lab. Syst.* 125 (2013) 18–32.
- [24] C. Chang, et al., Application of a weighted Grey-Taguchi method for optimizing recycled aggregate concrete mixtures, *Cement Concr. Compos.* 33 (10) (2011) 1038–1049.
- [25] H.-S. Shih, D.L. Olson, TOPSIS and its Extensions: a Distance-based MCDM Approach, vol. 447, Springer, 2022.
- [26] W.-C. Yang, et al., Materials selection method using improved TOPSIS without rank reversal based on linear max-min normalization with absolute maximum and minimum values, *Mater. Res. Express* 9 (6) (2022) 065503.
- [27] C.-L. Hwang, et al., *Methods for multiple attribute decision making*. Multiple Attribute Decision Making: methods and Applications a state-of-the-art, Surveyor (1981) 58–191.
- [28] R.K. Roy, A Primer on the Taguchi Method, Society of manufacturing engineers, 2010.